

## CHAPTER - III

### MATERIALS AND METHODS

---

---

#### 3.1 Materials

The chemicals which are used for this study are of analytical grade, purchased from Sigma Aldrich, India. The chemicals are analytical grade, hence used without any further purification. The oil (Mahuwa oil) was procured from local oil extracting factories, which has a composition of palmitic acid 24.5 %, stearic acid 22.7%, oleic acid 37.0 %, linoleic acid 14.3 % (Trifed, 2013). Double distilled water is used for the preparation and dilutions of all solutions.

#### 3.2 Preparation of green multi-metal catalyst

The stems of *Alternanthera sessilis* is used for the preparation of multi-metal catalyst as per the following procedures. The *Alternanthera sessilis* stems were collected after the removal of the leaves, air dried for about one week, the stems were cut into small pieces with a mean size of 2 to 5 cm. The cut stems are carbonized in nitrogen atmosphere using muffle furnace at a temperature of 750°C for 1 h. The carbonized stem of *Alternanthera sessilis* were washed few times with distilled water and finally with alcohol. The washed material was finally dried in a hot air oven at 105°C for 24 h (Murugesan at al., 2017).

#### 3.3 Synthesis of NCB

The carbonized stems of *Alternanthera sessilis* were soaked with mahuwa oil for about 30 min. The oil soaked stems were air dried for about

1h. The oil loaded *Alternanthera sessilis* stems were kept on a stainless steel grill and it is burnt from the bottom using LPG gas as a fuel mixed with air as shown in the Fig. 3.1. The oil loaded stems along with the Mahuwa oil start to burn at its ignition temperature, then the fuel gas (LPG) was cut off and the air inlet is regulated in such a way that, the combustion temperature was controlled at 420 to 470°C.

During the combustion, a soot is formed, which is then collected over the combustion chamber using a dome shaped surface of chromium oxide layer of Stainless steel lid (316SS). Exhaust vents were provided to allow the passage of excess flue gas. The ash formed during the combustion process was frequently removed through the discharge opening provided at the bottom of the reactor. The NCB deposited at the inner surface of stainless steel dome was collected using a sharp and thin scrubber. The collected NCB was washed with double distilled water and finally with alcohol.

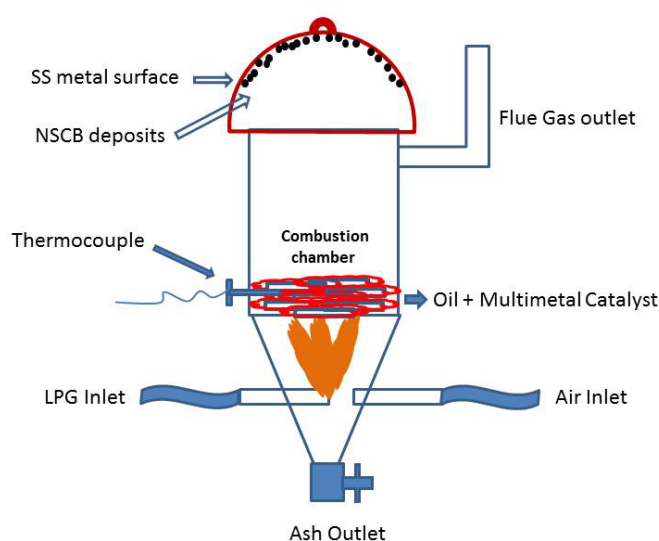


**Fig. 3.1 – CVD reactor assembly for the synthesis of NCB**

### **3.4 Activation of NCB using microwave oven**

The carbon balls collected in the above process was stirred with minimum quantity of 4 N nitric acid and made into a paste. The paste is kept in microwave oven and activated at 600 w for 5 min. Finally the activated NCB was washed with double distilled water for 4 times and an alcohol, then dried in a hot air oven for 2 h at 105°C and finally used for further studies (Tamilselvi, 2015).

### **3.5 Synthesis of Ferric oxide doped NCB (Fe<sub>3</sub>O<sub>4</sub>@NCB)**

Exactly 100 ml of 0.1M solution of FeCl<sub>3</sub>.6H<sub>2</sub>O was mixed with 0.5 g of activated NCB and stirred with magnetic stirrer for about 30 min. Then 1:1 ammonia was added drop wise with this mixture with constant stirring. The gel formation takes place at a pH of 8.0. After the gel formation, the ammonia addition was stopped and the contents were continuously stirred for another 4h. Then, the carbon doped with Fe was carefully filtered, washed, dried in hot air oven at 110°C for 24h and then finally calcined at 400°C for 1h under constant flow of nitrogen at 0.1 bar. The calcined Fe<sub>3</sub>O<sub>4</sub>@NCB magnetic composite was cooled to room temperature and stored in tight lid container for further studies.

### **3.6 Characterization**

The surface morphology was examined using field emission scanning electron microscope (FE-SEM) ZEISS (Alagappa University, Karaikudi, India) at an accelerating voltage of 5 kV. The NCB and the composite nanoparticles were characterized by powder X-ray diffraction (PANalytical X'Pert PRO powder X-ray Diffractometer, Alagappa University, Karaikudi,

India) equipped with Cu-K  $\alpha$  ( $\lambda = 1.54 \text{ \AA}$ , 40 kV, 30 mA, 40kV and step width 0.05 degree). The XRD data recorded for a  $2\theta$  range of 10.02 to 80.92° with a scan step time of 10.16 s. Other physico chemical parameters of the adsorbent as well as the characteristics of effluent samples were evaluated using the procedure given by Sivakumar (2009).

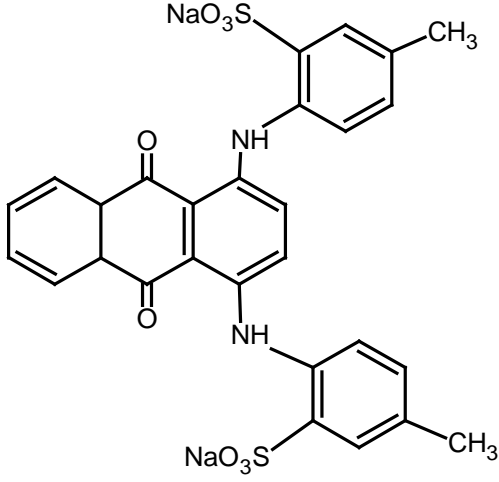
### 3.7 Batch Adsorption studies

Three types of dyes were selected for the evaluation of the adsorption characteristics of  $\text{Fe}_3\text{O}_4@\text{NCB}$  under batch and column mode. The molecular structure and the properties of the selected dyes are given in table 3.1.

**Table 3.1 - Molecular structure and the properties of selected dyes**

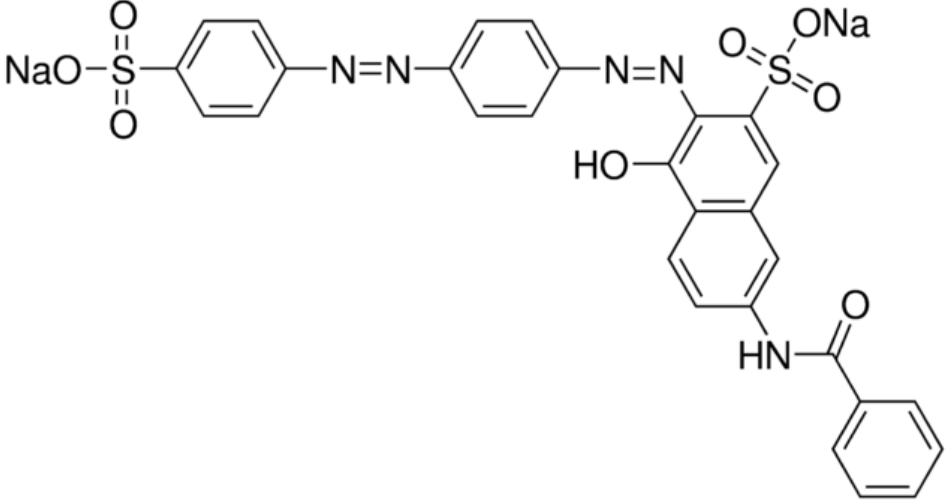
Methylene Blue	Properties	
	Molecular weight	319
	Molecular formula	$\text{C}_{16}\text{H}_{18}\text{ClN}_3\text{S}\cdot 2\text{H}_2\text{O}$
	C.I No.	52015
	Absorption maxima	665 nm

<b>Acid Green 25</b>	<b>Properties</b>	
	Molecular weight	622.58
	Molecular formula	$C_{28}H_{20}N_2Na_2O_8S_2$
	C.I No.	61570
Absorption maxima	642 nm	

The chemical structure of Acid Green 25 is a naphthoquinone derivative. It features a central naphthoquinone core with two amine groups (-NH-) at the 1 and 8 positions. Each amine group is attached to a 3,5-dimethyl-4-sulfonatephenyl ring. The sulfonate groups are represented as NaO<sub>3</sub>S, and the methyl groups are represented as CH<sub>3</sub>.

<b>Direct Red 81</b>	<b>Properties</b>	
	Molecular weight	675.60
	Molecular formula	$C_{29}H_{19}N_5Na_2O_8S_2$
	C.I No.	28160
Absorption maxima	508 nm	

The chemical structure of Direct Red 81 is a complex azo dye. It consists of a central azo group (-N=N-) connecting two benzene rings. The left benzene ring has a sodium sulfonate group (-SO<sub>3</sub>Na) at the para position. The right benzene ring is substituted with a sodium sulfonate group (-SO<sub>3</sub>Na) at the para position, a hydroxyl group (-OH) at the ortho position, and an amide group (-NH-CO-Ph) at the other ortho position, where Ph represents a phenyl ring.

A stock solution of 1000 mg/L of the respective dye was prepared using appropriate amount of dye (based on the percentage of purity) dissolved in distilled water. This stock solution was diluted as and when required. For the batch mode adsorption studies, 100 mL of dye solution of specified concentration was agitated with 100 mg of Fe<sub>3</sub>O<sub>4</sub>@NCB composite in 250 mL reagent bottle (Borosil-R glass bottles) fitted with tight lids. The contents were shaken using REMI make orbital shaker, which has temperature controller units. For the effect of pH, the dye solutions were added with required amount of 1M HCl and 1M NaOH solutions. After the specified time of agitation, the contents of the flask were centrifuged using universal make centrifuge at 5000 rpm and the final concentration of the dye solution was estimated by measuring the absorbance at the λ<sub>max</sub> of the respective dye solution using UV-VIS spectrometer (Model : Elico-BL198). All the adsorption experiments were done in duplicate (to minimize the variations of human and environmental factors) and the maximum deviations from the two runs are 4% only.

The percentage and amount of dye removed through adsorption was calculated using the following relationships.

$$\text{Percentage of dye removed} = \frac{\text{Initial concentration}(C_0) - \text{Concentration at time } t (C_t)}{\text{Initial concentration } (C_0)} \times 100$$

Amount of dye removed per unit weight of adsorbent (q<sub>t</sub>)

$$= (C_0 - C_t) \frac{V}{W} \text{ mg/g}$$

Where, V is the volume of dye solution in mL and W is the weight of adsorbent in grams.

### 3.8 Column Adsorption studies

Large scale industrial operations require the evaluation of any new adsorbent to be tried in column mode adsorption studies also. The fixed bed reactor was designed in laboratory scale using glass column of 1.2 cm diameter and 40 cm height. The adsorbent is packed over a porous silica dick kept at the bottom of the column and the top is covered with glass wool. The dye solution is fed from the bottom using a peristaltic pump in an up flow method in-order to ensure proper contact between the solute and sorbent. The treated solution coming out of the column was analyzed for the residual dye concentration using UV-VIS spectrometer (Model: Elico-BL198) as stated above.

### 3.9 Mathematical models used in this study

#### 3.9.1 Pseudo-first order kinetic model

A first order equation suggested by Lagergren (1898) for the sorption of liquid/solid system based on solid capacity. The pseudo-first order model proposed by Lagergren can be represented as:

$$\frac{d_q}{d_t} = k_1(q_e - q_t) \quad (3.1)$$

where,  $q_e$  is the amount of solute adsorbed at equilibrium (mg/g),  $q_t$  is the amount of solute adsorbed at time 't' (mg/g),  $k_1$  is the pseudo-first-order rate constant ( $\text{min}^{-1}$ ) and 't' is time (min).

The eqn. (3.1) is integrated for the boundary conditions  $t = 0$  to  $t = t$  and  $q = 0$  to  $q = q_t$ , gives

$$\log(q_e - q_t) = \log q_e - \frac{k_1}{2.303}t \quad (3.2)$$

A plot of “log(q<sub>e</sub>-q<sub>t</sub>)” and “t” will give a linear trace provided the adsorption follows first order kinetics. The values of k<sub>1</sub> and q<sub>e</sub> can be determined from the slope and intercept.

### 3.9.2 Pseudo-Second Order Kinetics

When an adsorption does not follow first order, the liquid phase adsorption of solute can also be described by pseudo-second order kinetic model (Ho and McKay, 1999). The pseudo-second order kinetic model is represented as:

$$\frac{dq}{dt} = k_2(q_e - q_t)^2 \quad (3.3)$$

Integrating eqn. (3.3) for the boundary conditions

t = 0 to t = t and q<sub>t</sub> = 0 to q<sub>t</sub> = q<sub>e</sub>, gives

$$\frac{1}{(q_e - q_t)} = \frac{1}{q_e} + k_2t \quad (3.4)$$

Where, k<sub>2</sub> is the pseudo-second order rate constant (g/mg/min). The eqn. (3.4) can be rearranged to obtain a linear form:

$$\frac{t}{q_t} = \frac{1}{k_2q_e^2} + \frac{1}{q_e}t \quad (3.5)$$

The initial adsorption rate, h (mg/g/min), as t → 0 can be defined as

$$h = k_2q_e^2 \quad (3.6)$$

A plot of “time” vs “t/q<sub>t</sub>” will give a linear trace, when the adsorption follows second order. The values of q<sub>e</sub> and k<sub>2</sub> were calculated from the slope and intercept of the above said plot.

### 3.9.3 Elovich Model

Elovich proposed a kinetic model to describe the chemisorption kinetics of gas adsorption onto solids (Cheung et al., 2000). The linear form of Elovich equation was derived from the basic Elovich kinetic equation:

$$\frac{dq_t}{dt} = \alpha e^{-\beta q_t} \quad (3.7)$$

Integrating the eqn. (3.7) for the boundary conditions t = 0 to t = t and q<sub>t</sub>=0 to q<sub>t</sub>= q<sub>e</sub>, gives

$$q_t = \frac{1}{\beta} \ln(\alpha\beta) + \frac{1}{\beta} \ln(t + t_0) \quad (3.8)$$

where, α and β are the Elovich kinetic parameters of the equation and t<sub>0</sub> = 1/(αβ), α represents the rate of chemisorption at zero coverage (mg/g/min). Another constant β is related to the extent of surface coverage and activation energy for chemisorption (g/mg).

When t<sub>0</sub> << t, then equation (3.8) becomes

$$q_t = \frac{1}{\beta} \ln(\alpha\beta) + \frac{1}{\beta} \ln t \quad (3.9)$$

A plot of “q<sub>t</sub>” vs “ln t” will give the constants, α and β, from the slope and intercept.

### 3.9.4 Intra-particle Diffusion Model

The initial adsorption of any batch mode adsorption process occurs on the surface of the adsorbent. Along with the surface adsorption, there is a possibility of diffusion of the adsorbate into the interior pores of the adsorbent. Weber and Morris (1963) suggested a kinetic model to analyse, whether the given adsorption is intra particle diffusion or not. Based on their theory,

$$q_t = k_d \cdot t^{1/2} \quad (3.10)$$

Where,  $k_d$  is the rate constant for the intra particle diffusion, which can be calculated from the plot of “ $q_t$ ” vs “ $t^{1/2}$ ”.

### 3.10 Adsorption isotherm

The adsorption isotherms are established to describe the equilibrium existence of adsorbate between the liquid and solid phase. Experimental isotherm data collected for the adsorption of the selected dyes onto  $\text{Fe}_3\text{O}_4@\text{NCB}$  at different temperatures fit in Langmuir and Freundlich adsorption isotherm models.

#### 3.10.1 Langmuir Model

The isotherm model was basically developed for the demonstration of gas adsorption onto the surface of solid adsorbent. The model derived based on the assumption of monolayer adsorption and energetically homogeneous surface of adsorbent. The Langmuir (1918) isotherm model is;

$$q_e = \frac{Q_0 \cdot b_L \cdot C_e}{(1 + b_L \cdot C_e)} \quad (3.11)$$

On rearranging the eqn. (3.11) into linear form,

$$\frac{C_e}{q_e} = \frac{1}{Q_0 \cdot b_L} + \frac{C_e}{Q_0} \quad (3.12)$$

Where,  $b_L$  is the Langmuir isotherm constant,  $C_e$  is the equilibrium concentration of the selected dye in solution,  $C_0$  is the initial concentration of the selected dye (mg/L) and  $Q_0$  is a Langmuir monolayer adsorption capacity. The constants  $Q_0$  and  $b_L$  can be calculated from the slope and intercept of the plot of " $C_e/q_e$ " Vs " $C_e$ ".

The essential characteristics of Langmuir isotherm can also be described by a dimensionless separation factor  $R_L$  which is defined by the following equation (Hall et al., 1966).

$$R_L = 1 / (1 + b_L \cdot C_0) \quad (3.13)$$

The value of separation factor  $R_L$  indicates the nature of the adsorption process as given below.

$$R_L > 1 \quad \rightarrow \text{Unfavorable}$$

$$R_L = 1 \quad \rightarrow \text{Linear}$$

$$0 < R_L < 1 \quad \rightarrow \text{Favorable}$$

$$R_L = 0 \quad \rightarrow \text{Irreversible}$$

### 3.10.2 Freundlich Model

The Freundlich (1906) isotherm model is an empirical equation which can be used for non-ideal sorption that involves heterogeneous sorption. The Freundlich isotherm can be derived based on the assumption that the increase

in the fraction of occupied sites will lead to a logarithmic decrease in the enthalpy of sorption. The original Freundlich non-linear equation is:

$$q_e = k_f C_e^{1/n} \quad (3.14)$$

On linearizing the eqn. (3.14), we get

$$\log q_e = \log k_f + \frac{1}{n} \log C_e \quad (3.15)$$

where,  $k_f$  is related to adsorption capacity and  $n$  is related to intensity of adsorption. The Freundlich constants,  $k_f$  and  $n$  were calculated from the linear plot of “ $\log q_e$ ” Vs “ $\log C_e$ ”

When  $1/n$  is  $>1.0$ , the change in adsorbed dye concentration is greater than the change in the solute concentration.

### 3.11 Thermodynamics of Adsorption

The thermodynamic parameters, which govern the adsorption process such as Gibbs free energy change  $\Delta G^\circ$ , standard enthalpy  $\Delta H^\circ$  and standard entropy  $\Delta S^\circ$  were also evaluated to analyze the role of temperature on the adsorption process. These parameters were calculated based on the isotherm data collected for 50 mg/L of respective dye solution under the range of selected temperatures. The thermodynamic parameters were evaluated using the following mathematical relationship.

$$\Delta G^\circ = -RT \ln b_L \quad (3.16)$$

$$\ln b_L = \frac{\Delta S^\circ}{R} - \frac{\Delta H^\circ}{RT} \quad (3.17)$$

Where,  $b_L$  is the Langmuir isotherm constant,  $C_{ads}$  is the amount of dye (mg/L) adsorbed onto  $Fe_3O_4@NCB$  at equilibrium,  $C_{sol}$  is the equilibrium concentration of dye (mg/L) in the solution,  $T$  is the solution temperature in K and  $R$  is a gas constant. The values  $\Delta H^\circ$  and  $\Delta S^\circ$  were evaluated from the slope and intercept of Vant Hoff plot of  $\ln b_L$  Vs  $1/T$ .

### **3.12 Column Mode Analysis**

Full scale column operation at the industrial level can be designed on the basis of results derived at laboratory scale. For the evaluation of efficiency and applicability of the column models, many mathematical models have been proposed in the past for the large-scale operations. The breakthrough curve or concentration-time profile and adsorption capacity of the adsorbent for the selected adsorbate are necessary to predict the column performance under the given set of operating conditions. Many models have been developed to predict the adsorption breakthrough behavior with high degree of accuracy. Thomas (1944) and Yoon-Nelson (1984) models are used in this study to analyze the behavior of the selected adsorbent-adsorbate system under the given set of operating conditions.

#### **3.12.1 Thomas Model**

Prediction of the concentration-time profile or breakthrough curve for the effluent is highly essential for the successful design of a column adsorption process. Thomas (1944) model is used for the calculation of the adsorption rate constant and the solid phase concentration of the dye on the  $Fe_3O_4@NCB$  surface using the column adsorption studies. Thomas kinetic model has the following form

$$\frac{C_t}{C_0} = \frac{1}{1 + \exp\left[\frac{k_T (q_{0(T)} \cdot m - C_0 \cdot v)}{r}\right]} \quad (3.18)$$

Where,  $C_t$  is effluent dye concentration at time,  $t$  (mg/L),  $C_0$  is initial dye concentration (mg/L),  $k_T$  is Thomas rate constant, (L/min.mg),  $q_{0(T)}$  is maximum dye adsorption capacity (mg/g),  $m$  is mass of  $\text{Fe}_3\text{O}_4@\text{NCB}$  (g),  $v$  is effluent volume (mL) and  $r$  is flow rate (mL/min). The value of time,  $t = v/r$ .

The constants  $k_T$  and  $q_{0(T)}$  were determined from a plot of “ $C_t/C_0$ ” against “ $t$ ” using non-linear regression analysis.

### 3.12.2 Yoon-Nelson Model

Yoon and Nelson (1984) have proposed a less complicated model to represent the breakthrough of gases onto activated charcoal. The model is proposed based on the assumption that the rate of decrease in the probability of adsorption for each adsorbate molecule is proportional to the probability of adsorbate adsorption on the adsorbent. The linear form of Yoon-Nelson model is

$$\ln\left(\frac{C_t}{C_0 - C_t}\right) = k_{YN} \cdot t - \tau \cdot k_{YN} \quad (3.19)$$

where,  $k_{YN}$  is Yoon-Nelson rate constant,  $\tau$  is the time required for 50% of

adsorbate breakthrough and  $t$  is the sampling time. A plot of  $\ln\left(\frac{C_t}{C_0 - C_t}\right) V_S$  “ $t$ ” gives a straight line with a slope of  $k_{YN}$  and intercept of  $-\tau \cdot k_{YN}$ .

Based on Yoon-Nelson model, the amount of dye being adsorbed in a fixed bed is half of the total dye entering the adsorption bed within  $2\tau$  period.

For a given bed

$$q_{0(YN)} = \frac{q_{(total)}}{m} = \frac{\frac{1}{2} C_0 [(r/1000) \times 2\tau]}{m} = \frac{C_0 \cdot r \cdot \tau}{1000m} \quad (3.20)$$

From this equation, the adsorption capacity,  $q_{0(YN)}$  varies as a function of inlet dye concentration ( $C_0$ ), Flow rate ( $r$ ), weight of adsorbent ( $m$ ) and 50% breakthrough time.

### 3.13 Error analysis

The adsorption capacity of  $Fe_3O_4@NCB$  obtained by the various mathematical models was compared with that of the experimental adsorption capacity using the following Error analysis method.

$$Sd = \sqrt{\sum \frac{(q_{0(exp)} - q_{0(cal)})^2}{N}} \quad (3.21)$$

Where,  $q_{0(exp)}$  is experimental adsorption capacity,  $q_{0(cal)}$  is the adsorption capacity calculated using theoretical kinetic models and  $N$  is the number of experimental points run.